

Ab initio calculation of the origin of the distortion of α -PbO

G. W. Watson* and S. C. Parker

Computational Solid State Chemistry Group, Department of Chemistry, University of Bath, Claverton Down, Bath, BA2 7AY, United Kingdom

G. Kresse

Institut für Theoretische Physik, Technische Universität Wien, Wiedner Hauptstraße 8-10, A-1040 Wien, Austria

(Received 15 July 1998)

We present *ab initio* calculations using density-functional theory (DFT) within the local density approximation (LDA) on PbO in the α phase and the idealized CsCl structure. The calculated structure of the α phase, which is predicted to be the most stable, is in good agreement with experiment. It has a nonspherical electron distribution forming what could be described as sterically active lone pair formed by the $6s^2$ electrons. However, analysis of the partial density of states reveals mixing of the Pb $6s$ with the oxygen $2p$ electronic states indicating that the classical theory of hybridization of the lead $6s$ and $6p$ orbitals is incorrect and that the “lone pair” is the result of the lead-oxygen interaction. [S0163-1829(99)05913-5]

INTRODUCTION

Lead oxide displays a number of polymorphs including a low-temperature tetragonal (α) phase¹ and a high-temperature orthorhombic (β) phase,² which both show significant distortions around the lead sites. It is often assumed that the distortions of lead oxide polymorphs are the result of the $6s^2$ electrons forming a lone pair which is sterically active and associated with the classical view of orbital hybridization. However, the presence of such electron pairs does not necessarily result in distorted structures. For example, although PbO forms a number of distorted phases with asymmetric Pb sites, PbS is cubic, forming a NaCl-type lattice with perfectly symmetric Pb sites.³

Previous theoretical studies have been performed on PbO structures but these have mainly been based on semiempirical quantum mechanics⁴⁻⁶ in which empirically fitted parameters are required and relaxation of the atomic sites is not usually performed. Trinquier and Hoffmann⁵ performed a comprehensive study of the band structure and bonding of PbO units starting from dimers, building up to layers and finally the three-dimensional solids of both α - and β -PbO. They showed the possibility of direct Pb-Pb bonding between the layers (stronger in α than β) although in contrast to experiment their calculations predicted that the β phase was more stable than the α phase.

One *ab initio* study has been performed⁷ but again the unit cells were fixed at the experimentally determined structures during the band-structure calculation. None of the previous studies allowed optimization of the structural parameters and were thus unable to compare the distorted structures of PbO with related undistorted structures which would allow direct investigation of the origin of the distortion.

The aim of this work is to study the electron distribution in α -PbO and the idealized CsCl structured PbO using a fully *ab initio* technique embodied in the density-functional theory (DFT) program VASP (Refs. 8-10) (Vienna *Ab initio* Simulation Package). These structures were chosen because α -PbO is the thermodynamically stable phase at room

temperature¹ and can be described as a distorted CsCl structure. The tetragonal α -PbO structure can be thought of as the CsCl structure with an elongated c axis. The layer of lead atoms is split in half forming a layered structure shown by Figs. 1(a) (CsCl) and 1(b) (α -PbO). Both the lead and oxygen are four coordinate in α -PbO, rather than eight coordinate as found in CsCl. The oxygen atoms are at the center of a distorted tetrahedra with all four coordinating oxygens on the same side of the lead.

THEORETICAL METHODS

We have employed the *ab initio* density-functional theory (DFT) method as implemented in the code VASP (Refs. 8-10) to study CsCl structured PbO and α -PbO. The Kohn-Sham equations¹¹ were solved self-consistently using an iterative matrix diagonalization method. This is based on a band-by-band preconditioned conjugate gradient^{8,12} method with an improved Pulay mixing^{9,13} to efficiently obtain the ground-state electronic structure. The forces on the atoms and the stress tensor were calculated using the Hellmann-Feynman theorem and used to perform a conjugate gradient relaxation. This was continued until the forces on the atoms had converged to less than 0.01 eV/Å and the pressure on the cell had equalized (a , b , and c are allowed to relax within the constraint of constant volume).

The calculations were performed within periodic boundary conditions allowing the expansion of the crystal wave functions in terms of a plane-wave basis set. The number of plane waves required to represent the oscillations of the valence orbitals near the core is prohibitive and thus we have used the pseudopotential approximation to represent the valence-core interactions. In this study we have employed ultrasoft Vanderbilt-type pseudopotentials^{14,15} (USPP) with all the electrons except the $6s^2$ and $6p^2$ of Pb considered to be part of the core and all except the $2s^2$ and $2p^4$ part of the oxygen core. Additional test calculations show that treating the Pb $5d$ electrons as valence electrons has only a small

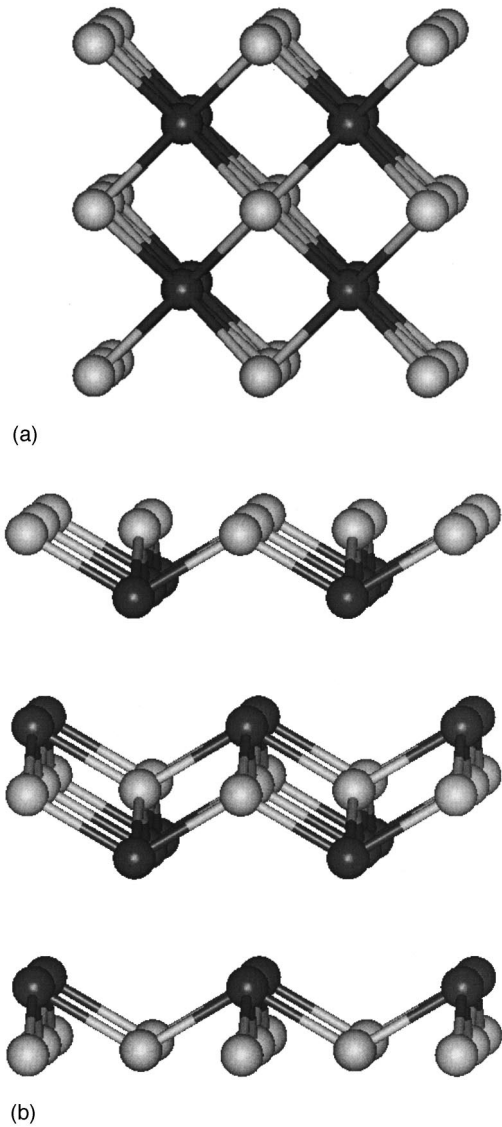


FIG. 1. Illustration of the structure of (a) CsCl structured PbO and (b) α -PbO. Lead atoms are dark while oxygen atoms are light.

effect on the atomic and valence electronic structure and will be detailed elsewhere.¹⁶

The exchange and correlation energy was evaluated within the local-density approximation (LDA) from the calculations of Ceperly and Alder¹⁷ using the parametrization of Perdew and Zunger.¹⁸ Although previous studies have indicated that methods based on gradient corrected functionals can give more accurate energies, we are primarily interested in the electronic structure rather than bond energies and thus the LDA is well suited for our purposes.

Convergence of the calculation was checked by calculating the equilibrium structure for a number of plane-wave energy cutoffs and a number of k -point grids which will be detailed in the next section.

OPTIMIZATION OF THE LATTICE VECTORS

Calculations were performed with VASP for a series of volumes to obtain the energy as a function of volume. From these data the equilibrium lattice vectors and bulk modulus were obtained. Convergence of the calculation was checked

TABLE I. Convergence test results showing the variation in volume and binding energy (per formula unit) for CsCl PbO and α -PbO and a function of plane-wave cutoff.

Cutoff	CsCl PbO		α -PbO	
	Energy (eV)	Volume (\AA^3)	Energy (eV)	Volume (\AA^3)
300	-9.457	30.176	-10.309	38.246
400	-9.454	30.168	-10.308	38.137
500	-9.456	30.167	-10.310	38.148

with respect to both the plane-wave cutoff and the number of k points, which were obtained using the Monkhorst-Pack¹⁹ method. For the metallic CsCl structured PbO, the linear tetrahedron method with quadratic corrections according to Blochl²⁰ was used to evaluate the total energy.

We have calculated the effect of the plane-wave cutoff on the energy and equilibrium lattice vectors by evaluating the variation of the energy as a function of volume for three cutoffs 300, 400, and 500 eV. For these calculations we used a k -point sampling grid of $8 \times 8 \times 8$ for the CsCl structure and $6 \times 6 \times 6$ for the α -PbO. The equilibrium volume and the energy for each cutoff are shown in Table I. The results clearly show that the calculations were well converged with a cutoff of 400 eV, illustrating that the use of ultrasoft pseudopotentials allows accurate calculations to be performed for oxides with a modest plane-wave cutoff energy. To ensure accuracy all of the following calculations have been performed at a cutoff of 400 eV.

A similar test was used to evaluate the k -point sampling required. Using the chosen cutoff of 400 eV we performed calculations at three different k -point grids for each of the structures, $6 \times 6 \times 6$, $8 \times 8 \times 8$, and $10 \times 10 \times 10$ for cubic PbO and $4 \times 4 \times 4$, $6 \times 6 \times 6$, and $8 \times 8 \times 8$ for α -PbO (Table II). The calculations were well converged even with the intermediate grids, so that further calculations were performed using k -point grids of $8 \times 8 \times 8$ for CsCl PbO and $6 \times 6 \times 6$ for α -PbO.

The results of the equilibrium structures and properties at a cutoff of 400 eV and k -point sampling of $8 \times 8 \times 8$ for cubic PbO and $6 \times 6 \times 6$ for α -PbO are given in Table III along with experimental data where available. The binding energies clearly show that the calculations predict that the

TABLE II. Convergence test results showing the variation in volume and binding energy (per formula unit) for CsCl PbO and α -PbO and a function of k -point sampling density.

K-point grid	CsCl PbO	
	Energy (eV)	Volume (\AA^3)
$6 \times 6 \times 6$	-9.452	30.201
$8 \times 8 \times 8$	-9.454	30.168
$10 \times 10 \times 10$	-9.454	30.172
	α -PbO	
$4 \times 4 \times 4$	-10.309	38.151
$6 \times 6 \times 6$	-10.308	38.137
$8 \times 8 \times 8$	-10.308	38.147

TABLE III. Comparison of calculated and experimental structural properties of PbO.

Property	CsCl	α phase	
	Calculated	Experimental	Calculated
Binding Energy (eV/Pb)	-9.454	-	-10.308
Volume ($\text{\AA}^3/\text{Pb}$)	30.168	39.272	38.137
a (\AA)	3.113	3.965	3.956
b (\AA)	-	3.965	3.956
c (\AA)	-	4.996	4.874
Pb (Z)	-	0.2368	0.2403
Pb-O distance (\AA)	8×2.696	4×2.32	4×2.285
K (GPa)	116.1	-	24.3

tetragonal α phase is more stable than the cubic CsCl structure as expected for the thermodynamically stable phase. The predicted lattice vectors and the only free internal coordinate (the Z coordinate) are in excellent agreement with experimental observations for the α phase. The a vector is underestimated by only 0.009 \AA , the c vector is underestimated by 0.122 \AA , and the z coordinate is underestimated by 0.0035. The underestimation of these parameters is typical for calculations performed within the local-density approximation. As is usual for LDA calculations the length of weak bonds, such as interaction between the Pb-O layers, is underestimated more significantly than that of strong bonds leading to a somewhat larger error for the c lattice vector. The rather weak bonding between the Pb-O layers is also responsible for the low bulk modulus (calculated by a fit to the volume squared around the equilibrium) of 24.3 GPa observed for α -PbO.

THE ELECTRON DENSITY

The electron densities calculated by VASP were displayed using INSIGHT II (Ref. 21) and are shown for slices through planes containing Pb atoms in Figs. 2(a) and 2(b) for the CsCl structured PbO and α -PbO. For CsCl structured PbO the electron density around the Pb is clearly spherical. In contrast, that of the α phase forms an enhanced density on the side of the Pb atom that points away from the PbO layers and towards each other. This asymmetric electron distribution could be attributed to the classical $6s^2$ lone pair which would thus be interpreted as directing the layered structure, i.e., stereochemically active. An interesting feature of this is that it effectively cuts down the lead-lead distance. If the lone pair position is defined as being centered at the maximum of the electron density the lone pair-lone pair distance (2.85 \AA) is substantially shorter than the lead-lead distance of either α -PbO (3.75 \AA) or CsCl structured PbO (3.11 \AA) and may indicate that lone pair-lone pair interactions are important in holding the layers together. Indeed, if the distances between lead atoms in metallic lead are used as a guide (3.47 \AA) then significant lead-lead interactions could be responsible for holding the layers together as suggested by Trinquier and Hoffmann.⁵

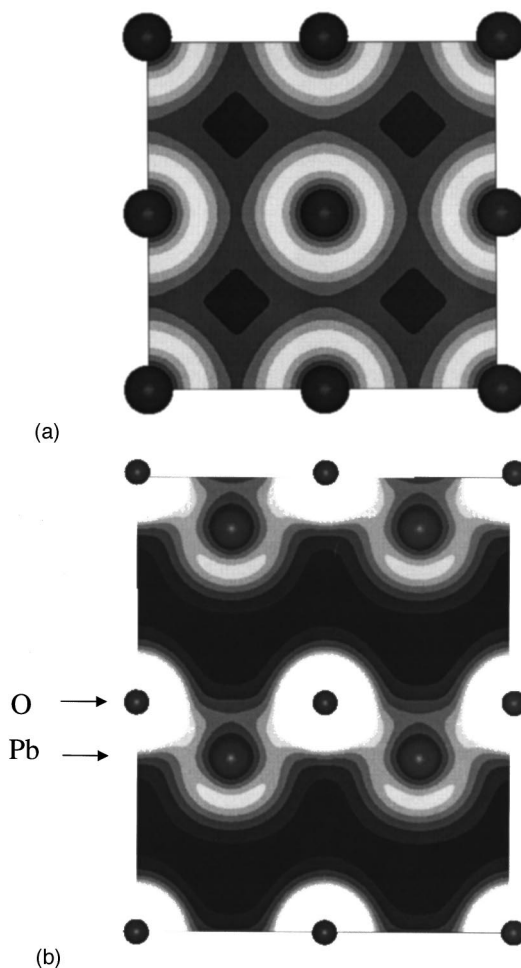


FIG. 2. Electron density contour plot through a plane containing lead atoms. (a) Spherical distribution around the lead atoms in CsCl structured PbO and (b) distribution in α -PbO showing the spherical-like electron density within the oxygen planes and the distorted distribution around the lead atoms below the oxygen planes. Contour levels are at 0.05 $e/\text{\AA}^3$ with black below 0.05 $e/\text{\AA}^3$ and white above 0.30 $e/\text{\AA}^3$.

THE ELECTRONIC STRUCTURE

The electronic density of states (EDOS) were calculated by sampling the Brillouin zone with a more dense grid of $19 \times 19 \times 19$ for the CsCl structure, and $13 \times 13 \times 13$ for the α -PbO. They are shown relative to the Fermi level in Figs. 3(a) and 4(a) for CsCl PbO and α -PbO with the band structures given in Figs. 3(b) and 4(b), respectively.

Whereas our calculations show that PbO is semimetallic in the CsCl structure, α -PbO exhibits an indirect band gap of approximately 1.00 eV. This value is significantly smaller than the experimental one of 1.95 eV at 300 K,²² however, it is well known that LDA has a tendency to underestimate band gaps. Previous band-structure calculations, using the augmented spherical wave method within the LDA, predicted a band gap of 1.82 eV.⁷ This is significantly closer to the experimental value than our calculations, however, the ASW method depends heavily on the size of the Wegner-Seitz radii used for each atom (and the addition spheres added for the void space). Their calculations show that as the oxygen atom size is increased and the lead decreased the band gap reduces. They employed a large lead to oxygen ratio (1.35)

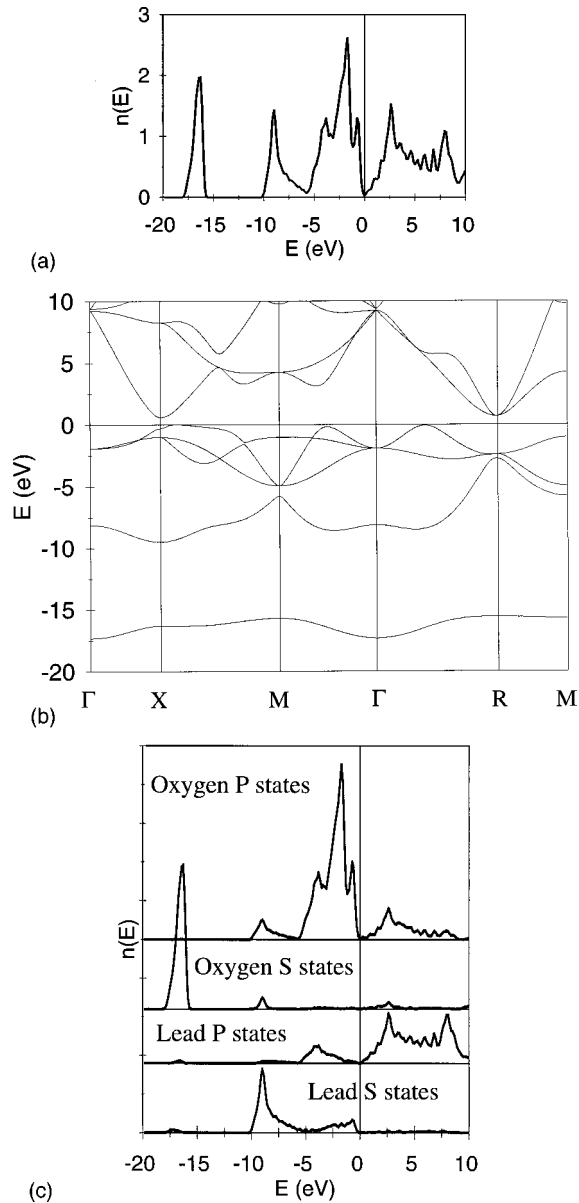


FIG. 3. Electronic structure of CsCl structure PbO. (a) electronic density of states, (b) band structure, and (c) partial electronic density of states.

which is inconsistent with the charge-density plots (Fig. 2) to obtain a band gap similar to experiment. We believe that if a lead to oxygen ratio consistent with the charge densities (less than 1.0) had been used a band gap similar to ours would have been obtained.

To simplify the interpretation of the electronic structure, we have also calculated the partial (ion and l-quantum number decomposed) electronic density of states (PEDOS). These were obtained by projecting the wave functions onto spherical harmonics centered around each atom [see Figs. 3(c) and 4(c)] with a radius of 1.55 Å for both atom types and both structures. These radii were chosen because they give rise to reasonable space filling, but the results (at least the qualitative aspects) are insensitive to a change of the radii.

The EDOS for both structures are remarkably similar with both exhibiting a low-lying O 2s peak (−18 to −16 eV).

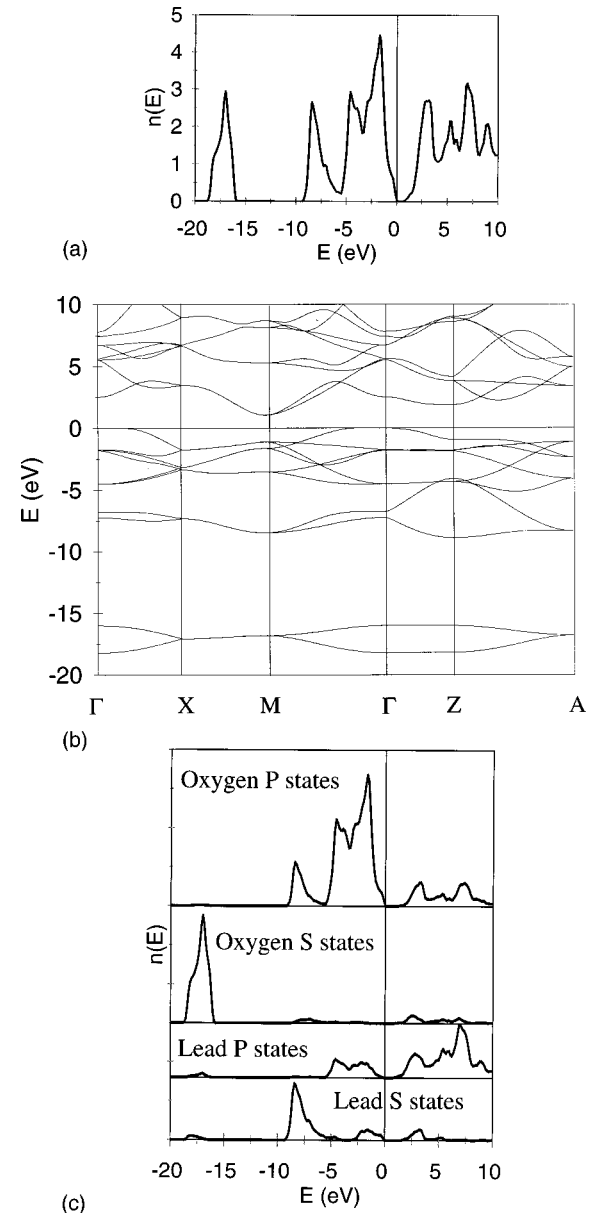


FIG. 4. Electronic structure of α -PbO. (a) electronic density of states, (b) band structure, and (c) partial electronic density of states.

They also both have a prominent peak between −10 and −5 eV which is derived mainly from the Pb 6s orbital. Finally, the third peak below the Fermi level is primarily due to the O 2p states with the Pb 6p orbitals responsible for the states above the Fermi level. In a simplified ionic picture one would expect that two electrons are transferred from the Pb to the O. The band structure and EDOS are in accord with this expectation with the O 2s and 2p derived bands both below the Fermi level, whereas for Pb only the 6s bands are occupied. However, the PEDOS indicates that this picture is oversimplified. In particular, the O 2p states are strongly hybridized with both the Pb 6s and Pb 6p. For example, approximately 30% of the charge density of the peak between −10 and −5 eV (Pb 6s peak) is derived from the O 2p orbitals. For a more thorough discussion we turn to the evaluated band structure.

The band structure of PbO in the CsCl structure is shown in Fig. 3(b). The first feature that comes immediately to at-

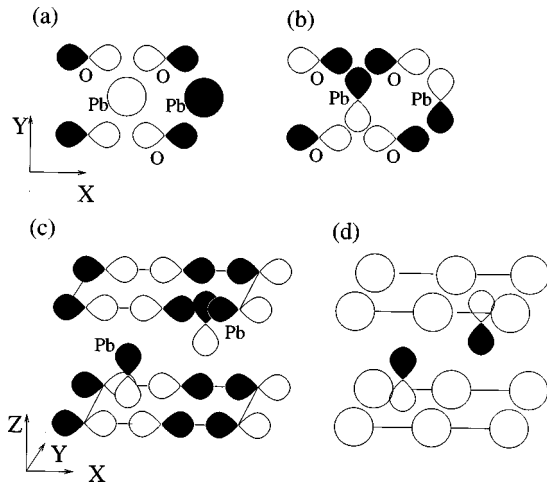


FIG. 5. Schematic representation of the orbital interactions which make up bonding and combinations. (a) O p_x /O p_y and Pb s , (b) O p_x /O p_y and Pb p_y , (c) O p_x /O p_y and Pb p_z , and (d) O s and Pb p_z .

tention is the anomalous dispersion of the Pb $6s$ band along the line gamma X. For an s -derived band one would usually expect the energy to increase along this direction (as it does for the O- s -derived band) due to the change from an in-phase interaction with adjacent unit cells at gamma, to an out-of-phase interaction at X. This anomalous behavior is related to the strong hybridization of the Pb $6s$ band with the oxygen $2p$ bands. This hybridization is strongest at the X point where the phase in neighboring cells is exactly opposite. The O p_x orbital can therefore interact strongly with the Pb s orbital with the corresponding bonding linear combination shown in Fig. 5(a). This results in the Pb s band moving down in energy and the O p_x band up in energy. The latter behavior is particularly important because it gives rise to the closing of the gap in the vicinity of the X point and it is also responsible for the high density of states just below the Fermi level. There is also some hybridization between the O $2p$ and the Pb $6p$ orbitals as can be seen in the PEDOS, but due to symmetry this interaction is limited to few k points only. For example, no effective hybridization can occur between the O $2p$ and Pb $6p$ orbitals at the Γ or M point. However at the R point the O $2p$ and Pb $6p$ states can form a bonding and antibonding linear combination as indicated in Fig. 5(b), so that the highest energy valence bands are shifted in energy away from Fermi level at the R point.

To conclude bonding in CsCl is mainly ionic, although there is also some covalent bonding caused by a hybridization of O $2p$ and Pb $6p$ states. However, the most important feature of the band structure of PbO in the CsCl structure is the strong hybridization of the Pb s and O p orbitals. This interaction gives rise to a significant contribution to the electronic states just below the Fermi level and is also responsible for the Pb s contribution to the EDOS at the top of the valence band. Energetically this interaction does not gain or require any energy because both states (Pb $6s$ and O $2p$) are located below the Fermi level. However, it is clear that energy could be gained if these states hybridize more efficiently with the unoccupied Pb $6p$ states so that the O $2p$ bands move down in energy away from the Fermi level (bonding-antibonding splitting).

In α -PbO, for which the band structure is shown in Fig. 4(b), this type of interaction does occur. The lowest two bands (there are now two oxygens per primitive cell) are derived again from the O $2s$ orbitals, the next two bands from the Pb $6s$ orbitals, then a complex of four bands is visible, which is mainly due to O p_x and O p_y orbitals (i.e., the oxygen p orbitals oriented parallel to the PbO layer). The final two bands just below the Fermi surface are mainly due to O p_z states. The bands above the Fermi surface are again derived from the Pb $6p$ orbitals. The crucial question is why this structure is more stable than the CsCl one. An important clue is that, in contrast to the CsCl structure, in the α -PbO the O p_x and O p_y states do not contribute to the density of states below the Fermi level. In fact, as we will elaborate below, these orbitals can interact very efficiently with the Pb p_z orbitals, stabilizing the α -PbO structure.

In Fig. 2(b) the charge density around the Pb site was shown to be considerably distorted, with charge accumulation in the z direction. If the EDOS is decomposed according to the magnetic quantum numbers, it is found that the Pb p_z orbital has, in agreement with the charge-density contour plots, an increased occupancy compared to the Pb p_x and Pb p_y orbitals. The reason for this is that due to the displacement of the Pb atoms, the Pb p_z orbital can interact more efficiently with the O $2p_x$ and O $2p_y$, (i.e., those states close to the Fermi level in CsCl structured PbO). To illustrate this we again draw attention to the O $2p_x$ derived states at the top of the valence band in Figure 5(b). In the CsCl structure, these orbitals interact only with the Pb s orbitals [see Fig. 5(a)] because the symmetry does not allow for an interaction with the Pb p_z orbitals [as indicated in Fig. 5(c), the interaction with the top layer has the opposite sign than that with the bottom layer]. In the α -PbO, half of the Pb atoms have moved in the $+z$ direction and half of them in the $-z$ direction, breaking the symmetry and allowing hybridization between the indicated linear combination of O orbitals and the Pb p_z orbital. As a result some of the O p_x O p_y derived states (in fact those that had the strongest interaction with the Pb s state) are lowered in energy and move away from the Fermi surface effectively counterbalancing the destabilization caused by interaction with the Pb s orbital. This stabilizes the α phase as the increase in the antibonding states is now in the unoccupied levels. The only bands that cannot profit from this type of interaction are the O $2p_z$ derived ones, which for this reason are located just below the Fermi level. In passing we note that the Pb $6p_z$ states can also interact more efficiently with the O $2s$ states in the α -PbO structure, as shown in Fig. 5(d). But the energy gain due to this bonding-antibonding interaction is likely to be very small.

In summary, the electronic structure of PbO indicates that a strong interaction of the Pb $6s$ and O $2p$ states occurs giving rise to bonding and antibonding combinations which are both filled. The antibonding states occur at the top of the valence bands and account for the contribution of Pb s states to the EDOS just below the Fermi level in the CsCl structure. The distorted phase is more stable because it decreases the density of states below the Fermi level by allowing for a more efficient hybridization between the occupied O $2p$ and unoccupied Pb $6p$ orbitals. Our analysis shows that it is this interaction (and not the hybridization of Pb $6s$ and Pb $6p$

orbitals) which gives rise to the distorted electron density around the Pb. This picture of the electronic structure is at variance with the classical view of hybridization of the lead $6s$ with the $6p$ orbitals as the Pb $6s$ states are clearly contributing directly to covalent bonding with oxygen. In addition it is also clear that the O p states are directly involved with the formation of the distorted electron distribution.

CONCLUSIONS

We have demonstrated the use of *ab initio* calculations based on density-functional theory to examine the electronic structure of CsCl structure PbO and α -PbO. The calculations show excellent reproduction of the structure of α -PbO and indicate that the electron distribution around the lead is heavily distorted in contrast to the results on CsCl structured PbO. This distorted electron distribution could be interpreted as a classical sterically active hybridized lone pair, however, analysis of the detailed electronic structure reveals a more complicated picture.

The partial electronic density of states indicated that the main interaction of the Pb $6s^2$ electrons is with the oxygen $2p$ states and not with the lead $6p$, thus the lone pair is not the result of classical hybridization. In the CsCl structure a

strong interaction between the Pb s and O p orbitals pushes some of the O $2p$ bands, for instance those in the vicinity of the X point, towards the Fermi level. This interaction can be counterbalanced in the α -PbO structure where the Pb $6pz$ orbitals interact with exactly the same states in a bonding-antibonding fashion, which results in a large energy gain.

The distorted electron distribution was shown to be primarily caused by a mixing of the O $2p$ with Pb $6p$ and some Pb $6s$ and contradicts the classical view of hybridization. This is consistent with the observation that PbS does not form a distorted Pb site, which would also seem to be at odds with the Pb hybridization theory, as the formation of the ‘‘lone pair’’ is dependent on the energies of the valence states on Pb and the anion in question. From this it is clear that an anion with valence states of differing energies to O may be unable to interact in the same way to form the asymmetric electron distribution. Calculations are currently underway to calculate the electronic structure of PbS.

ACKNOWLEDGMENTS

We would like to thank EPSRC for financial support and Molecular Simulations, Inc. for the provision of INSIGHT II.

*Present address: Department of Chemistry, University of Wales, Cardiff, PO Box 912, Cardiff CF1, UK. Electronic address: watsongw1@cardiff.ac.uk

¹J. Leciejewicz, Acta Crystallogr. **14**, 1304 (1961).

²J. Hill, Acta Crystallogr., Sect. C: Cryst. Struct. Commun. **41**, 1281 (1985).

³A. R. H. F. Ettema, C. Haas, P. Moriarty, and G. Hughes, Surf. Sci. **287**, 1106 (1993).

⁴G. A. Bordovskii, N. L. Bordeev, A. N. Ermoshkin, V. A. Izvozchikov, and R. A. Evarstov, Phys. Status Solidi B **115**, K15 (1983).

⁵G. Trinquier and R. Hoffmann, J. Phys. Chem. **88**, 6696 (1984).

⁶R. A. Evarstov and V. A. Veryazov, Phys. Status Solidi B **165**, 401 (1991).

⁷H. J. Terpstra, R. A. de Groot, and C. Haas, Phys. Rev. B **52**, 11 690 (1995).

⁸G. Kresse and J. Hafner, Phys. Rev. B **49**, 14 251 (1994).

⁹G. Kresse and J. Furthmüller, Comput. Mater. Sci. **6**, 15 (1996).

¹⁰G. Kresse and J. Furthmüller, Phys. Rev. B **54**, 11 169 (1996).

¹¹W. Khon and L. J. Sham, Phys. Rev. **136**, B864 (1965).

¹²M. C. Payne, M. Teter, D. C. Allen, T. A. Arias, and J. D. Joannopoulos, Rev. Mod. Phys. **64**, 1045 (1992).

¹³P. Pulay, Chem. Phys. Lett. **73**, 393 (1980).

¹⁴D. Vanderbilt, Phys. Rev. B **41**, 7892 (1990).

¹⁵G. Kresse and J. Hafner, J. Phys.: Condens. Matter **6**, 8245 (1994).

¹⁶G. W. Watson, S. C. Parker, and G. Kresse (unpublished).

¹⁷D. M. Ceperley and B. J. Alder, Phys. Rev. Lett. **45**, 566 (1980).

¹⁸J. Perdew and A. Zunger, Phys. Rev. B **23**, 5048 (1981).

¹⁹H. J. Monkhorst and J. D. Pack, Phys. Rev. B **13**, 5188 (1976).

²⁰P. Blöchl, O. Jepsen, and O. K. Anderson, Phys. Rev. B **49**, 16 223 (1994).

²¹INSIGHT II Graphical simulation package, Molecular Simulation, Inc. (1996).

²²R. C. Keezer, D. L. Bowman, and J. H. Becker, J. Appl. Phys. **39**, 2062 (1968).